

SUPPLEMENTAL MATERIAL (Poly(A)-specific ribonuclease is a nuclear ribosome biogenesis factor involved in human 18S rRNA maturation; Montellese et al. 2017)

Supplemental Table 1

List of primers used for site-directed mutagenesis, *in vitro* transcription and RNase H assays

PARN-1_siMut forward	5'-CTCCAGCATCGATTTCTTAGCAAGCC-3'
PARN-1_siMut reverse	5'-CTCTGACAAACAAATTTGACATCTGGTG-3'
PARN-H377A forward	5'-CAACTTGCCGAGGCAGGC-3'
PARN-H377A reverse	5'-TTCAGAGGCTGTGTCATAACTTGAAAAAC-3'
OHA416	5'-GGGCCGGATCCTAATACGACTCACTATAGGGTTCCGTAGGTGAACCTGCGGAAGG-3'
OHA418	5'-GGCGGAAGCTTGCAGTGGCGGTGGGGGGTGGGTGTGCGGAGGG-3'
ITS1-Hs-RACE	5'-CGCGAATTCGATCATTAACGGAGCCCGGAG-3'
RNaseH_1	5'-TTTACTTCTCTAGATAGTCAAGTTCGACC-3'
RNaseH_2	5'-TGTTACGACTTTTACTTCTCTAGATAGTC-3'

Supplemental Table 2

List of target genes and siRNA sequences used in the present study

Gene	GenBank accession #	siRNA	siRNA sequence
<i>PARN</i>	NM_002582.3	siPARN-1	5'-GCUCCAGCAUUGACUUUCUdTdT-3'
		siPARN-3	5'-GCAGAAACAUGCCAAAGAAAdTdT-3'
		siPARN-5	5'-AAGCUAUCGGAUCCAAACCUAdTdT-3'
		siPARN-6	5'-AGGACCAGACUUGCAGCCUAAAdTdT-3'
<i>NOB1</i>	NM_014062.2	siNOB1-1Q	5'-CGCCCUGGAGCCAAUCUUCAdTdT-3'
		siNOB1-2Q	5'-UUGCCCAACAUCGAUCAUGAAAdTdT-3'
		siNOB1-3	5'-AAGGUUAAGGUGAGCUCAUCGdTdT-3'
<i>PAPD5</i>	NM_001040284.2	siPAPD5-5	5'-GGACGACACUCAAUUUUdTdT-3'
		siPAPD5-6	5'-GGCCUUUGAUUAUGCCUACGUUGUdTdT-3'
<i>PAPD7</i>	NM_006999.4	siPAPD7-3	5'-CGCCGAAAGUACUUUAGGAdTdT-3'
		siPAPD7-5	5'-CCACCACUCCAGAACACUGAUCAUdTdT-3'
<i>LSG1</i>	NM_018385.2	siLSG1	5'-AGACCAAACUGGAACCAA-3'
<i>eIF6</i>	NM_001267810.1	siEIF6	5'-GAGCUUCGUUCGAGAACA-3'
<i>CRM1</i>	NM_003400.3	siCRM1	5'-UGUGGUGAAUUGCUUAUAC-3'
<i>ENP1</i>	NM_004053.3	siENP1	5'-AGCGTGCCATAGAGATGTT-3'
<i>CK1δ</i>	NM_001893.4,	siCK1δ	5'-CCATCGAAGTGTGTGTAA-3'
<i>CK1ε</i>	NM_001894.4	siCK1ε	5'-ACATCGAGAGCAAGTTCTA-3'
<i>RIO2</i>	NM_018343.2	siRIO2	5'-GGAUCUUGGAUAUGUUUA-3'
<i>LTV1</i>	NM_032860.4	siLTV1	5'-UGGCAGUGAUCUCCUAAA-3'
<i>RPS2</i>	NM_002952	siRPS2-2	5'-CCAGGUUCAAGGCAUUUGUdTdT-3'

<i>RPS3</i>	NM_001005	siRPS3-2	5'-CCAGGACAGAAAUCAUUAUdTdT-3'
<i>RPS10</i>	NM_001014	siRPS10-1	5'-GAACCGGAUUGCCAUUUAUdTdT-3'
<i>RPS11</i>	NM_001015	siRPS11-1	5'-GCGCCACAAGAACAUGUCUdTdT-3'
<i>RPS15</i>	NM_001018	siRPS15-2	5'-UCACCUACAAGCCCGUAAAdTdT-3'
<i>RPS17</i>	NM_001021	siRPS17-2	5'-GCAGGUUAUGUCACGCAUCdTdT-3'
<i>RPS21</i>	NM_001024	siRPS21-1	5'-GGAUGGGUGAGUCAGAUGAdTdT-3'
<i>RPS23</i>	NM_001025	siRPS23-1	5'-GGGUCCAGCUGAUCAAGAAAdTdT-3'
<i>RPS24</i>	NM_033022	siRPS24-1	5'-CACCGGAUGUCAUCUUUGUdTdT-3'
<i>RPS26</i>	NM_001029	siRPS26-1	5'-GGACAAGGCCAUUAAGAAAdTdT-3'
<i>RPS29</i>	NM_001032	siRPS29-1	5'-CGGUCUGAUCCGGAAAUAUdTdT-3'

Supplemental Table 3

List of probes used in Northern blot

5'ETS	5'-AGACGAGAACGCCTGACACGCACGGCAC-3'
5'ITS1	5'-CCTCGCCCTCCGGGCTCCGTTAATGATC-3'
ITS1-38	5'-GGAGGGAAGCGCGCGGCGGC-3'
ITS1-49	5'-GGTGGGTGTGCGGAGGGAAG-3'
ITS1-59	5'-GCGGTGGGGGGGTGGGTGTG-3'
ITS2-1	5'-CTGCGAGGGAACCCCCAGCCGCGCA-3'
ITS2-2	5'-GCGCGACGGCGGACGACACCGCGGCGTC-3'
18S	5'-TTTACTTCCTCTAGATAGTCAAGTTCGACC-3'
28S	5'-CCCGTTCCTTGGCTGTGGTTTCGCTAGATA-3'

Legends of the Supplemental Figures

Supplemental Figure S1: Endo- and exonucleolytic cleavages during pre-ribosomal RNA processing in human cells

This schematic representation summarizes the endo- and exonucleolytic steps undertaken in human cells to release ribosomal RNA sequences, as reported in the literature and described in the present study. Separation between pre-40S and pre-60S precursors occurs after endonucleolytic cleavage at site 2. Cleavage at site E releases the last 18S precursor, 18S-E pre-rRNA, corresponding to the sequence of 18S rRNA flanked in 3' by a portion of ITS1, 78 or 81 nt in length. This full-length precursor is referred to as 18S-E_{FL} pre-rRNAs in the present study. In the cytoplasm, 18S-E precursors are poly-uridylylated by an uncharacterized TUTase and processed into shorter pre-rRNAs¹. These precursors are then finally cleaved by the endonuclease NOB1, which releases the 18S rRNA 3' end^{1,2}. Upon knockdown of PARN, 18S-E_{FL} precursors can be exported to the cytoplasm and further processed, although less efficiently. Concerning the large ribosomal subunit pathway, two 5.8S rRNAs varying by 5 nt in their 5' extremity are produced (5.8S_L and 5.8S_S), although it is not known whether the longest form is obtained through endonucleolytic cleavage as in *Saccharomyces cerevisiae*. So far, the 3'-5' exoRNase ER11, acting on cytoplasmic 6S precursors, has only been described in

¹ Preti, M., O'Donohue, M.F., Montel-Lehry, N., Bortolin-Cavaille, M.L., Choismel, V. and Gleizes, P.E. (2013) Gradual processing of the ITS1 from the nucleolus to the cytoplasm during synthesis of the human 18S rRNA. *Nucleic acids research*, **41**, 4709-4723

² Sloan, K.E., Mattijssen, S., Lebaron, S., Tollrvey, D., Pruijn, G.J. and Watkins, N.J. (2013) Both endonucleolytic and exonucleolytic cleavage mediate ITS1 removal during human ribosomal RNA processing. *The Journal of cell biology*, **200**, 577-588.

mouse cells³. Several exoRNases, such as XRN2 or RRP6, are also involved in the degradation of transcribed spacers released after endonucleolytic cleavages.

Supplemental Figure S2: Assessment of the functionality of HAST-tagged PARN and PARN H377A

(A) Nuclear localization of PARN assessed with an anti-PARN antibody. PARN labeling is mainly seen in nucleoli (Nol), but a weaker signal is also seen in the nucleoplasm (Np). White arrowheads indicate the putative positions of a few fibrillar centers, which correspond to unlabeled areas. Scale bar, 5 μ m. (B) IF analysis of PARN after depletion of the export factor CRM1 (positive control) and 60S RBFs (LSG1, eIF6). Scale bar, 20 μ m. (C) Western blot analysis shows the efficiency of the knockdowns shown in Fig. 1F. (D) IF using an anti-HA antibody revealed that the intracellular localization of HAST-tagged PARN (w.t.) is similar to that of endogenous PARN displayed in (A). Similar results were obtained when HAST-tagged PARN was silently mutated to be insensitive to the action of the siRNA PARN-1 (siMut), or further mutated to provide a catalytically-dead form of the enzyme (HAST-PARN-H377A). (E) Purification of pre-40S particles with HAST-tagged PARN (w.t.) or HAST-tagged PARN-H377A led to similar profiles after silver staining.

Supplemental Figure S3: Western blot analysis of HeLa cells expressing HAST-tagged version of PARN and PARN H377A

As displayed on Figure 2E, HeLa cells treated with a scramble siRNA or siRNA PARN-1 were rescued with plasmids allowing expression of either an HAST-tagged version of PARN silently mutated to render it insensitive to siRNA PARN-1 (pPARN), or a catalytically inactive PARN mutant (pPARN-H377A). The empty plasmid (pHAST) was used as a control. Total protein samples were analyzed by Western blot and revealed with antibodies directed against PARN, the HA tag, or β -actin.

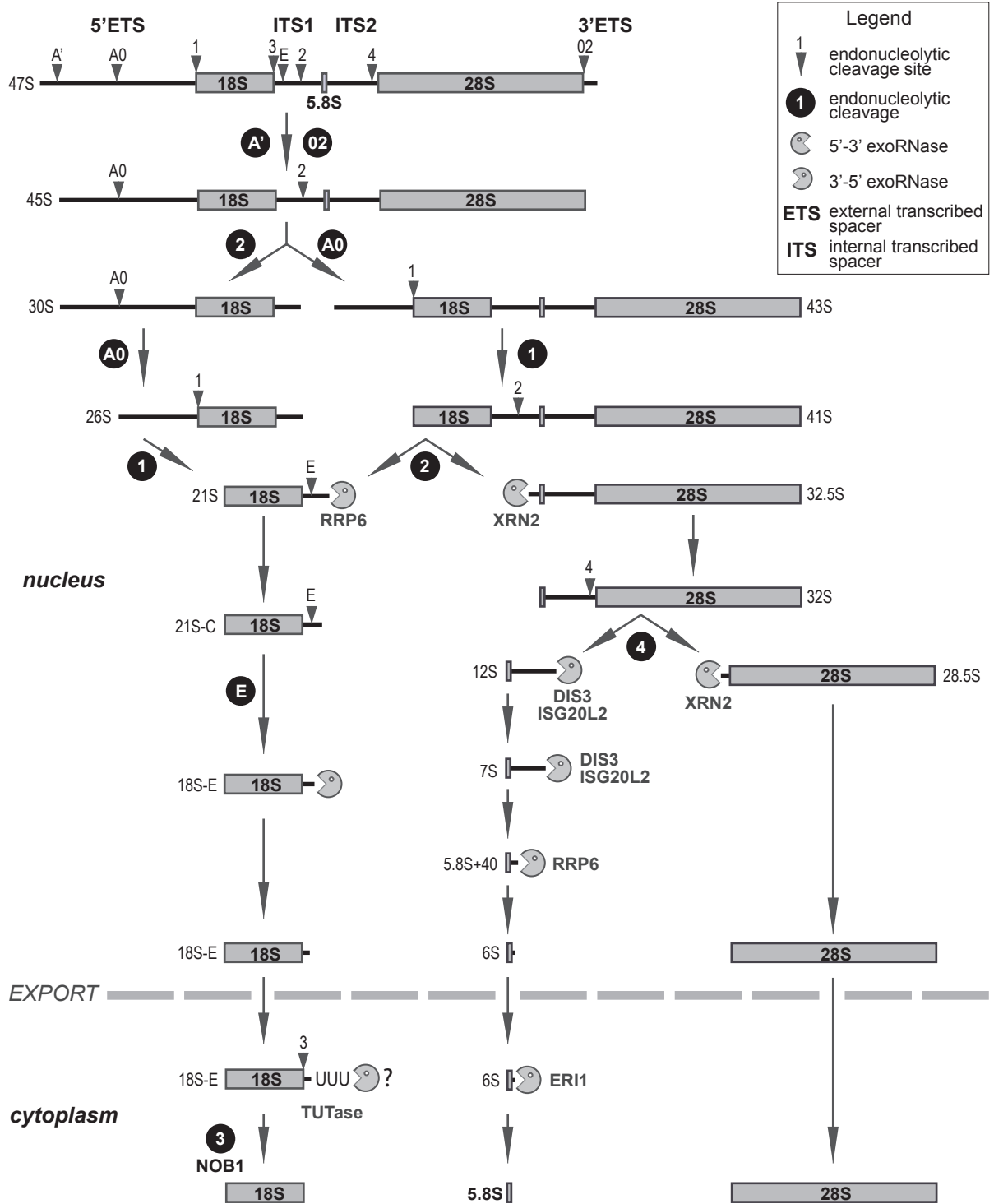
Supplemental Figure S4: Analysis of neo-synthesized RNAs in siRNA-depleted HeLa cells

In a parallel experiment to that presented on Fig. 2F, HeLa cells depleted of NOB1, or co-depleted of NOB1 and PARN, were pulse labeled with L-methyl ³H methionine. Cells were harvested and total RNAs were analyzed as described in the corresponding legend. The gel on the left is identical to that displayed on Fig. 2F.

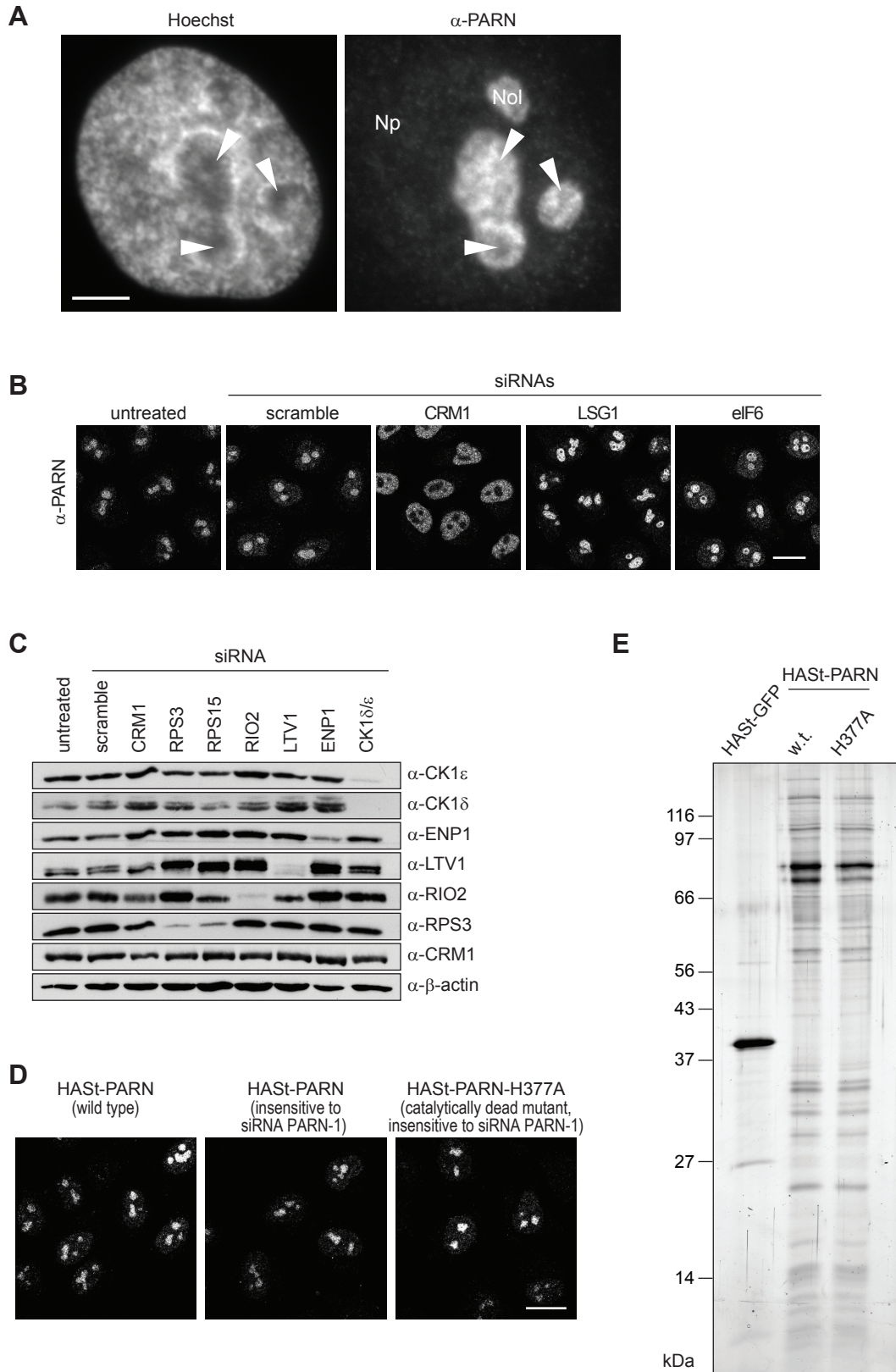
Supplemental Figure S5: Impact of PARN depletion on quality control

(A) Northern blot analyses of PARN co-depletion with RPSs that provoke an increase of 18S-E pre-rRNAs (see Fig. 4D for quantifications). (B) Northern blot analysis of RPS24, RPS23 or RPS11 depletions, which led to a strong accumulation of 30S pre-rRNAs, or of co-depletion of these RPSs with PARN. The graph presents the ratios of 30S pre-rRNA relative to 28S rRNA for each experimental condition. (C) An accumulation of abortive transcripts was induced by a low dose of actinomycin D in control cells and cells depleted of RPS26 or PARN, or co-depleted for RPS26 and PARN. Total RNAs were isolated after the indicated times and analyzed by Northern hybridization with 5'ITS1, ITS1-59 and 5'ETS probes.

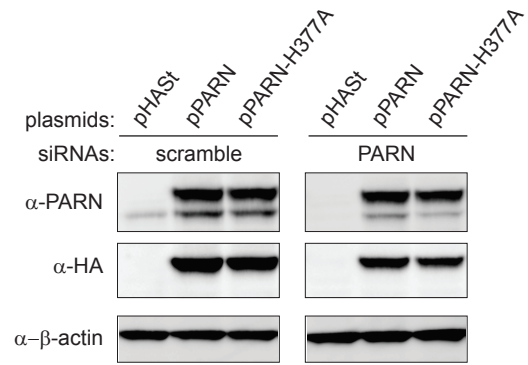
³ Ansel, K.M., Pastor, W.A., Rath, N., Lapan, A.D., Glasmacher, E., Wolf, C., Smith, L.C., Papadopoulou, N., Lamperti, E.D., Tahiliani, M. *et al.* (2008) Mouse Eri1 interacts with the ribosome and catalyzes 5.8S rRNA processing. *Nature structural & molecular biology*, **15**, 523-530.



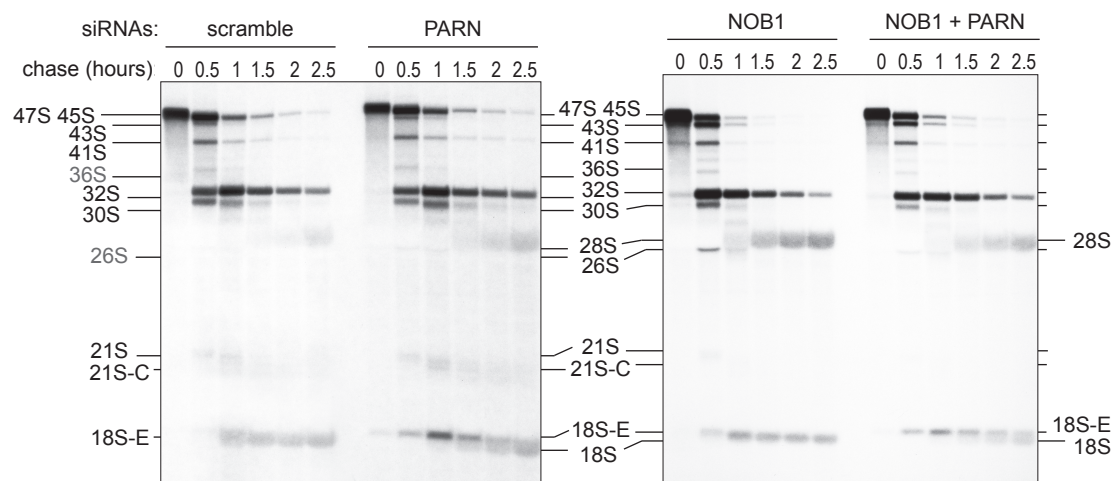
Supplemental Figure S1



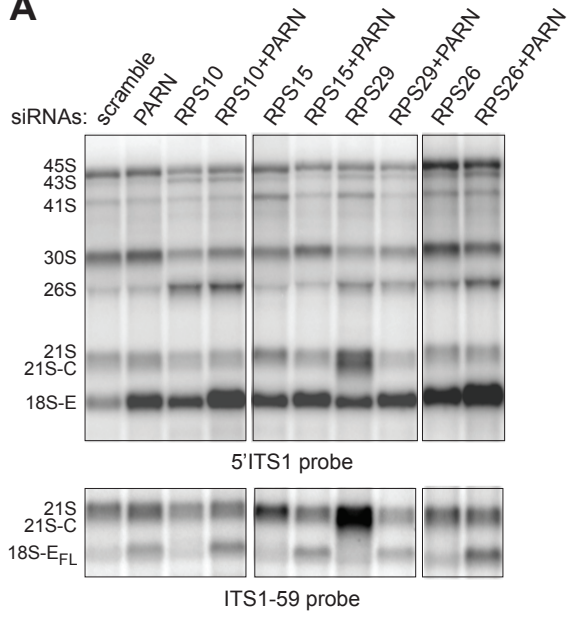
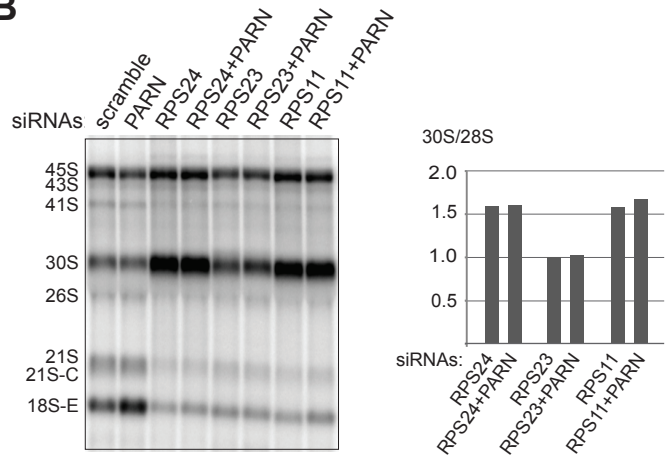
Supplemental Figure S2



Supplemental Figure S3



Supplemental Figure S4

A**B****C**